Differences and Correlations of Morphological and Hemodynamic Parameters between Anterior Circulation Bifurcation and Side-wall Aneurysms

Kai-kai GUO[1†], Chang-ya LIU[2†], Gao-hui LI[3], Jian-ping XIANG[3], Xiao-chang LENG[3], Yi-ke CAI[1], Xue-bin HU[1#]
[1]*Department of Neurosurgery, Union Hospital, Tongji Medical College, Huazhong University of Science and Technology, Wuhan 430022, China*
[2]*Department of Emergency, Longhua Hospital, Shanghai University of Traditional Chinese Medicine, Shanghai 200032, China*
[3]*Artery Flow Technology Co., Ltd., Hangzhou 310051, China*

[Abstract] Objective: The objective of this research was to explore the difference and correlation of the morphological and hemodynamic features between sidewall and bifurcation aneurysms in anterior circulation arteries, utilizing computational fluid dynamics as a tool for analysis. **Methods:** In line with the designated inclusion criteria, this study covered 160 aneurysms identified in 131 patients who received treatment at Union Hospital of Tongji Medical College, Huazhong University of Science and Technology, China, from January 2021 to September 2022. Utilizing follow-up digital subtraction angiography (DSA) data, these cases were classified into two distinct groups: the sidewall aneurysm group and the bifurcation aneurysm group. Morphological and hemodynamic parameters in the immediate preoperative period were meticulously calculated and examined in both groups using a three-dimensional DSA reconstruction model. **Results:** No significant differences were found in the morphological or hemodynamic parameters of bifurcation aneurysms at varied locations within the anterior circulation. However, pronounced differences were identified between sidewall and bifurcation aneurysms in terms of morphological parameters such as the diameter of the parent vessel (D_{vessel}), inflow angle (θ_F), and size ratio (SR), as well as the hemodynamic parameter of inflow concentration index (ICI) ($P<0.001$). Notably, only the SR exhibited a significant correlation with multiple hemodynamic parameters ($P<0.001$), while the ICI was closely related to several morphological parameters ($R>0.5$, $P<0.001$). **Conclusions:** The significant differences in certain morphological and hemodynamic parameters between sidewall and bifurcation aneurysms emphasize the importance to contemplate variances in threshold values for these parameters when evaluating the risk of rupture in anterior circulation aneurysms. Whether it is a bifurcation or sidewall aneurysm, these disparities should be considered. The morphological parameter SR has the potential to be a valuable clinical tool for promptly distinguishing the distinct rupture risks associated with sidewall and bifurcation aneurysms.
Key words: sidewall; bifurcation; unruptured aneurysms; computational fluid dynamics

Intracranial aneurysm (IA) is a serious cerebrovascular disease characterized by arterial wall thinning that leads to localized dilation. Approximately 85% of subarachnoid hemorrhages are caused by the rupture of IAs, resulting in severe disability or even death of the patient[1]. Given the lack of effective medications to prevent IA rupture, it is crucial that high-risk aneurysms are surgically treated as soon as they are detected. Endovascular embolization is one of the primary treatments for IAs[2].

Nonetheless, the potential complications associated with the management of unruptured aneurysms, coupled with the incidence of aneurysm rupture, render the clinical decision-making process for unruptured IAs exceedingly intricate. Consequently, the precise prediction of the rupture and recurrence risk of unruptured IAs retains substantial clinical importance. This can provide clinicians with the necessary knowledge to make judicious decisions on whether to initiate invasive interventions or adopt a vigilant surveillance strategy. Hemodynamics is a pivotal factor in the rupture of IAs, with computational fluid dynamics (CFD) serving as an invaluable instrument for assessing the development, rupture,

Kai-kai GUO, E-mail: m202175971@hust.edu.cn; Chang-ya LIU, E-mail: liuchangya198801@163.com
[†]These authors contributed equally to this work and share first authorship.
[#]Corresponding author, E-mail: 2006XH0856@hust.edu.cn

and recurrence of IAs. Numerous studies employing CFD have emphasized the influence of hemodynamics on the likelihood of IA rupture[2–5]. Yet, the majority of these studies have examined all IA subtypes in tandem, without differentiation between sidewall and bifurcation aneurysms, a potential confounding factor as noted by Hassan *et al*[6]. Furthermore, owing to the disparities in anatomical structure, the rupture risk is notably higher in bifurcation aneurysms than in sidewall aneurysms[7, 8]. Cerebral arteries bifurcate into anterior and posterior circulations, both of which exhibit considerable hemodynamic variances. Although aneurysms in the posterior circulation are more susceptible to rupture, they are less common and primarily bifurcation aneurysms. To mitigate potential bias, this study concentrated on aneurysms situated within the anterior circulation. We retrospectively compared two categories of aneurysms, sidewall and bifurcation aneurysms, in terms of their morphological and hemodynamic differences. In addition, we investigated the correlation between morphological and hemodynamic parameters of these two groups of aneurysms with the aim of identifying key parameters that can effectively differentiate rupture risk, thereby offering guidance for the therapeutic approach to IAs.

1 PATIENTS AND METHODS

1.1 Patient Selection

In this study, we conducted a systematic review of preoperative clinical data and arterial aneurysm imaging data for 146 patients treated at our hospital between January 2021 and September 2022. The data were analyzed using CFD. The inclusion criteria were as follows: (1) unruptured saccular aneurysm diagnosed via digital subtraction angiography (DSA); (2) aneurysm located within the anterior circulation; (3) availability of complete and high-quality DSA imaging data, suitable for accurate measurement of aneurysm morphology and representation of the IA and surrounding vascular system. The exclusion criteria were as follows: (1) recurrent aneurysm; (2) aneurysm situated within the posterior circulation; (3) IA with subpar neuroimaging data unsuitable for CFD simulation; (4) ruptured, traumatic, infectious, dissecting, and fusiform aneurysm, or aneurysm associated with other cerebrovascular diseases. Approval for this study was obtained from the Medical Ethics Committee of Tongji Medical College, Huazhong University of Science and Technology, China (No. S238). As the data were anonymized, the requirement for informed consent was consequently waived.

1.2 Classification of Aneurysms

Arterial aneurysms can be classified as sidewall aneurysms and bifurcation aneurysms based on the geometric shape of the parent artery. Sidewall aneurysms arise from a single parent artery or from a small branch originating from the aneurysm neck, whose diameter is less than 20% of the diameter of the parent artery. Bifurcation aneurysms are located at the division of cerebral arteries, and the diameter of any of the branching arteries is not less than 20% of the diameter of the parent artery[6, 8].

1.3 Vascular and Aneurysm Geometry Modeling

Pre- and postoperative DSA dicom files were obtained from GE workstations. Two groups of image data in DICOM format were imported into Materialise's Interactive Medical Image Control System software (MIMICS 20.01, Belgium) for image segmentation and reconstruction. The segmentation program mainly uses different segmentation methods to detect the optimal boundary of the artery surface. Finally, the obtained vascular model was converted into STL format. Then the reconstructed vessel model was imported into Geomagic Studio 15.0 (USA), the aneurysm and its parent artery were segmented manually, and the small branches of the parent artery were polished and smoothed. The STL files were saved in ASCII format for further analysis.

1.4 Morphological Assessments

Seven geometric parameters (fig. 1), including maximum height (H_{max}), perpendicular height (H), neck diameter (D_{neck}), parent vessel diameter (D_{vessel}), inflow angle (θ_F), aspect ratio (AR), and size ratio (SR), were measured by AneuFlow software (ArteryFlow Technology, China) and used to quantitatively compare the morphological characteristics between bifurcation and sidewall aneurysms.

1.5 Hemodynamic Simulation

The processed STL data were input into ANSYS 19.0 software (USA) for smoothing, grid creation, simulation calculation, and post-processing visualization. The software processing process was as follows: In order to ensure the accuracy of the simulation calculation, the maximum grid size was set as 0.2 mm, and the number of grids for the aneurysm model was one to two million after the completion of grid division. With a density of 1056 kg/m^3 and a viscosity of 0.0035 Pa·s, the blood was assumed to be a Newtonian fluid. Because the wall distensibility contributes minimally to the aneurysmal flow pattern, the aneurysm wall and vessel wall were assumed to be rigid with no-slip boundary conditions. The incompressible Navier-Stokes equations were numerically solved using an in-house finite elements solver. Since patient-specific blood flow information was not available, published mean flow rates and boundary waveforms were used as inlet boundary conditions for given vessel locations[9].

All simulations were conducted for up to 3 cardiac cycles and set at 800 steps per cardiac cycle with a time step of 0.001 s. We chose the last cycles as the output of the final analysis.

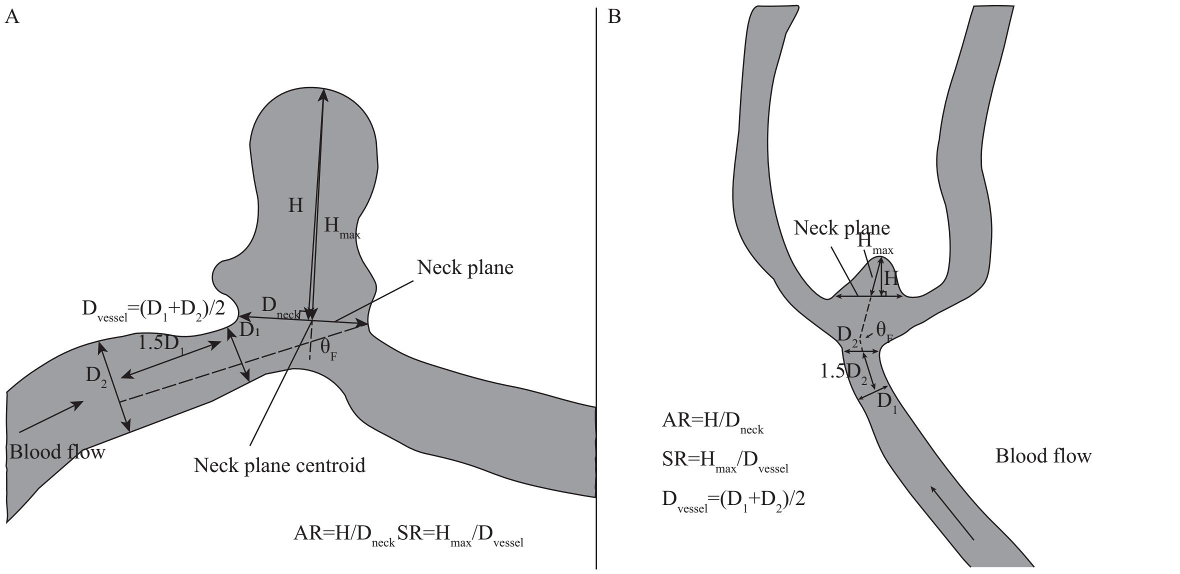

Fig. 1 Schematic diagram of morphological parameters of a sidewall aneurysm (A) and a bifurcation aneurysm (B)

1.6 Hemodynamic Comparison

Five typical hemodynamic parameters were used in our study: time-averaged wall shear stress (TAWSS), normalized wall shear stress (NWSS), oscillatory shear index (OSI), relative residence time (RRT), and inflow concentration index (ICI). NWSS was defined as the aneurysm wall shear stress (WSS) divided by the parent WSS. All parameters were calculated according to previous literature reports[10–13].

1.7 Statistical Analysis

Statistical analysis was performed using MedCalc 20.0 software (Belgium). The normality of quantitative data was evaluated by the Kolmogorov-Smirnov test. Normally distributed data are presented as the mean±standard deviation in the table, while non-normally distributed data are presented as median (P25, P75). We used the independent samples *t*-test (for normally distributed data) or the Mann-Whitney *U* test (for non-normally distributed data) to confirm the morphological and hemodynamic differences between the sidewall and bifurcation aneurysm groups. Pearson (for a normal distribution) or Spearman (for a skewed distribution) analysis was used to quantify the correlation between the morphological and hemodynamic characteristics of the sidewall and bifurcation groups. In addition, comparisons between the two models of geometric and hemodynamic parameters were performed between the middle cerebral artery (MCA) group and the anterior communicating artery (ACOM) group in bifurcated aneurysms. A *P*-value of less than 0.05 indicates a statistically significant difference.

2 RESULTS

2.1 Patients and IAs

During the investigation period, a total of 180 intracranial anterior circulation aneurysms were collected from 146 patients, consisting of 49 males and 97 females. These aneurysms were equally divided into two categories: 90 cases of sidewall aneurysms and 90 cases of bifurcation aneurysms. The average age of the patients afflicted with sidewall aneurysms was 56 years old, with an interquartile range of 51.00–63.50 years old. In contrast, the patients with bifurcation aneurysms had a mean age of 60 years old, with a standard deviation of 10.5 years old. The difference in age between the two groups was not statistically significant. The precise locations of these aneurysms are detailed in table 1.

Of the sidewall aneurysms, 78 (86.7%) were situated in the internal carotid artery (ICA), whereas of the bifurcation aneurysms, 41 (45.5%) were found in the MCA, and an equal number in the ACOM. Due to the limited sample size from other locations, we chose to exclude these samples to better emphasize the inherent patterns. Consequently, we obtained a total of 160 anterior circulation aneurysms from 131 patients. These aneurysms were then categorized into 3 groups for further analysis: sidewall ICA, bifurcation MCA, and bifurcation ACOM.

Table 1 Aneurysm locations and types

Location	*n*	Sidewall	Bifurcation
ICA	79	78	1
MCA	46	5	41
PCOM	4	2	2
ACOM	42	1	41
ACA	9	4	5
Total	180	90	90

ICA: internal carotid artery; MCA: middle cerebral artery; PCOM: posterior communicating artery; ACOM: anterior communicating artery; ACA: anterior cerebral artery

Table 2 Morphological and hemodynamic parameters of different aneurysms [mean±SD or median (IQR)]

Variable	Bifurcation MCA	Bifurcation ACOM	Sidewall ICA	*P*-value (MCA & ACOM)	*P*-value (ICA & MCA)	*P*-value (ICA & ACOM)
H_{max} (mm)	3.667 (2698–4.836)	3.687 (2.303–5.558)	3.143 (2.055–4.902)	0.849[b]	0.508[b]	0.667[b]
H (mm)	2.874 (2.307–4.437)	2.667 (1.937–4.357)	2.819 (1.725–4.111)	0.475[b]	0.454[b]	0.951[b]
D_{neck} (mm)	3.750±1.407	3.232 (2.823–4.098)	3.596 (2.877–4.798)	0.119[b]	0.627[b]	0.291[b]
D_{vessel} (mm)	2.1690±0.387	2.254±0.528	3.639±0.648	0.925[a]	<0.001[a]	<0.001[a]
θ_F (°)	130.333±22.337	136.200 (120.360–147.295)	86.355±27.096	0.878[b]	<0.001[a]	<0.001[b]
AR	0.780±0.326	0.779 (0.603–1.134)	0.704 (0.521–1.016)	0.867[b]	0.198[b]	0.179[b]
SR	1.633 (1.203–2.056)	1.465 (0.995–2.762)	0.955 (0.576–1.322)	0.739[b]	<0.001[b]	<0.001[b]
TAWSS	8.132±7.069	6.241±6.614	5.256 (4.036–7.376)	0.234[a]	0.050[b]	0.534[b]
NWSS	0.627±0.283	0.501 (0.373–0.807)	0.566 (0.436–0.832)	0.363[b]	0.689[b]	0.364[b]
OSI	0.009 (0.005–0.014)	0.006 (0.004–0.013)	0.007 (0.004–0.011)	0.288[b]	0.189[b]	0.927[b]
RRT	0.231 (0.119–0.422)	0.308 (0.154–0.607)	0.320 (0.201–0.437)	0.129[b]	0.094[b]	0.661[b]
ICI	1.458±0.934	1.054 (0.582–2.034)	0.500 (0.209–0.934)	0.439[b]	<0.001[b]	<0.001[b]

ICA: internal carotid artery; MCA: middle cerebral artery; ACOM: anterior communicating artery; H_{max}: maximum height; H: perpendicular height; D_{neck}: neck diameter; D_{vessel}: parent vessel diameter; θ_F: inflow angle; AR: aspect ratio; SR: size ratio; NWSS: normalized aneurysm wall shear stress; OSI: oscillatory shear index; RRT: relative residence time; ICI: inflow concentration index. [a]*T* test; [b]Mann-Whitney *U* test

2.2 Morphological and Hemodynamic Analyses

Table 2 presents a comparison of the morphology and quantitative hemodynamic parameters for the various aneurysms. It is evident that there were no significant differences in the morphological or hemodynamic parameters between bifurcation aneurysms at either location. Moreover, bifurcation aneurysms exhibited larger θ_F (P<0.001), SR (P<0.001), and ICI (P<0.001) values as well as a smaller D_{vessel} (P<0.001) than those of the sidewall aneurysms, as illustrated in the box plots (fig. 2). The remaining morphological parameters did not exhibit significant differences from the hemodynamic parameters.

Table 3 displays the correlations between the

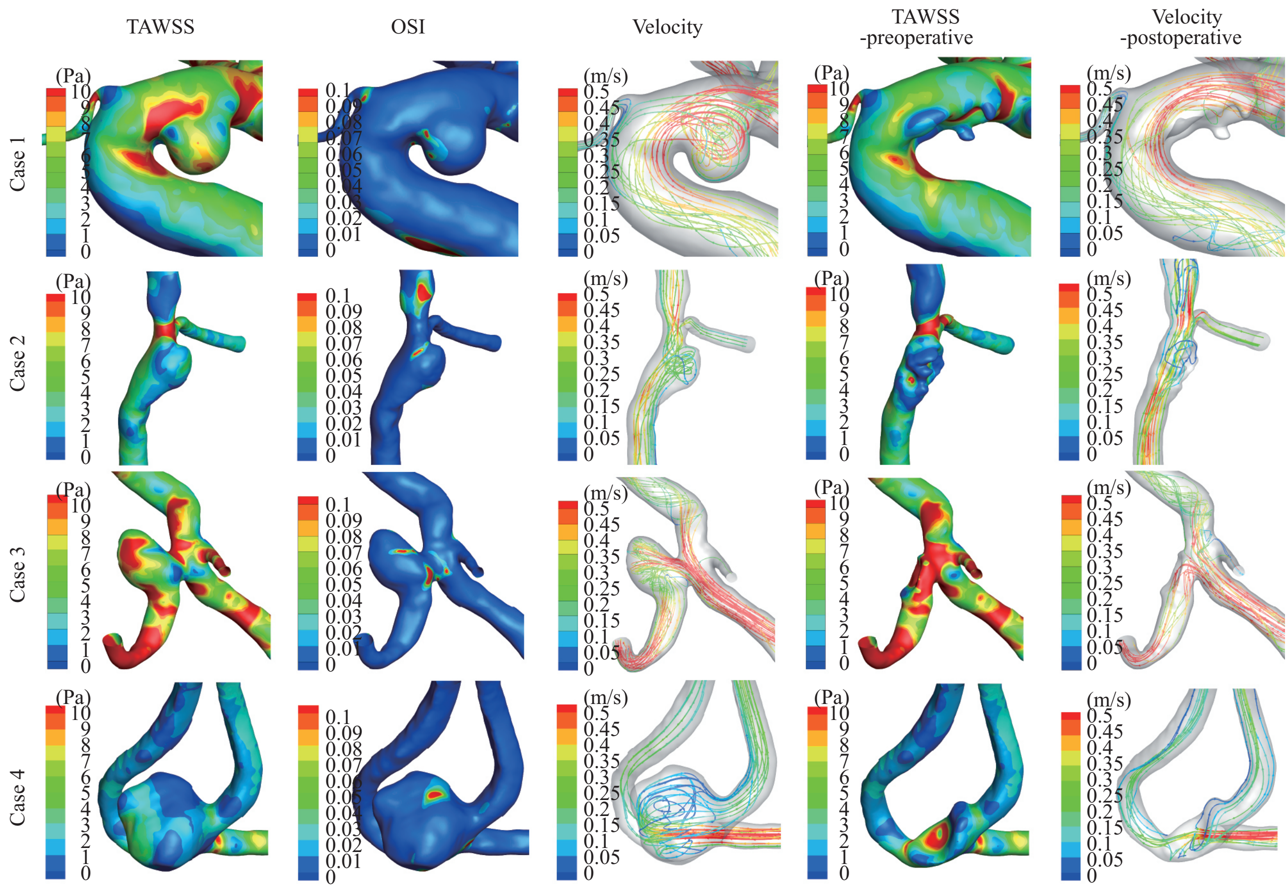

Fig. 2 Box plots showing the distributions of the parent vessel (D_{vessel}), inflow angle (θ_F), size ratio (SR), and inflow concentration index (ICI) for different aneurysms analyzed separately for the bifurcation and sidewall types

TAWSS: time-averaged wall shear stress; OSI: oscillatory shear index

Table 3 Correlations of morphological factors and hemodynamics among different aneurysm types

Sidewall aneurysm group					
Sidewall	TAWSS	NWSS	OSI	RRT	ICI
H_{max}	–0.2961*	–0.3831**	0.2367*	0.4157**	0.6851**
H	–0.3265*	–0.4097**	0.2344*	0.3804**	0.7027**
D_{neck}	–0.1966	–0.2324*	0.2170*	0.0651	0.7349**
D_{vessel}	–0.4307**	–0.0504	–0.0698	0.1080	–0.2866**
θ_F	–0.0430	–0.1289	0.1696	0.1245	0.1255*
AR	–0.2827*	–0.4454**	0.1755	0.5718**	0.3270**
SR	–0.1389	–0.3336*	0.3452**	0.5025**	0.6809**
Bifurcation aneurysm group					
Bifurcation	TAWSS	NWSS	OSI	RRT	ICI
H_{max}	–0.1950	–0.3257*	0.4020**	0.0744	0.6124**
H	–0.1471	–0.3231*	0.4054**	0.0661	0.6082**
D_{neck}	–0.1158	–0.0565	0.3374*	–0.0466	0.7254**
D_{vessel}	–0.2447*	0.1737	–0.0354	–0.0391	0.0663
θ_F	0.0509	–0.0656	0.3249*	–0.0927	0.2848*
AR	–0.1286	–0.4300**	0.2516*	0.1200	0.2856*
SR	–0.1091	–0.3598**	0.4159**	0.0635	0.5173**

H_{max}: maximum height; H: perpendicular height; D_{neck}: neck diameter; D_{vessel}: parent vesseldi-ameter; θ_F: inflow angle; AR: aspect ratio; SR: size ratio; NWSS: normalized aneurysm wall shear stress; OSI: oscillatory shear index; RRT: relative residence time; ICI: inflow concentration index. Note: Correlation coefficient (*R*)>0.8 indicates a particularly strong correlation; *R*=0.5–0.8 indicates a strong correlation; *R*=0.3–0.5 indicates a moderate correlation, and *R*<0.3 indicates a weak correlation. $^{*}P<0.05$, $^{**}P<0.001$

morphological and hemodynamic parameters for sidewall and bifurcation aneurysms. The bifurcation MCA aneurysm and bifurcation ACOM aneurysm parameters were not separately listed in table 3 because there were no significant differences between them. While most parameters exhibited correlations, only those with correlation coefficients greater than 0.5 were considered to have strong correlations, and those with correlation coefficients less than 0.5 represented moderate-to-weak correlations. Consequently, we selected only data with correlation coefficients greater than 0.5 to emphasize the patterns.

Several parameters of the sidewall and bifurcation aneurysms were significantly correlated with the ICI (*P*<0.001) [e.g., H_{max} (*R*s=0.6851, *R*b=0.6124), H (*R*s=0.7027, *R*b=0.6082), D_{neck} (*R*s=0.7349, *R*b=0.7254), and SR (*R*s=0.6809, *R*b=0.5173)]. Furthermore, each morphological parameter for sidewall and bifurcation aneurysms did not exhibit strong correlations with the NWSS or OSI (*R*>0.5).

In contrast, the RRT of sidewall aneurysms was significantly correlated with the AR (*R*s=0.5718) and SR (*R*s=0.5025) (*P*<0.001), while bifurcation aneurysms did not demonstrate this statistical correlation.

3 DISCUSSION

In the present investigation, we conducted a statistical analysis of the differences and associations between the morphological attributes of anterior circulation sidewall and bifurcation aneurysms as well as the traditionally acknowledged hemodynamic parameters influencing aneurysm rupture. Our aim was to identify key parameters capable of rapidly distinguishing the rupture risk of sidewall and bifurcation aneurysms, thereby facilitating the management of different IAs. The findings of this study revealed no considerable disparities in morphological or hemodynamic parameters among bifurcation aneurysms situated at different locations within the anterior circulation. However, significant differences were observed in morphological parameters such as D_{vessel}, θ_F, and SR as well as hemodynamic parameters like ICI between sidewall and bifurcation aneurysms, with SR being notably associated with several hemodynamic parameters. Moreover, no robust correlations were identified between TAWSS, NWSS, and OSI for each morphological parameter of sidewall and bifurcation aneurysms, whereas strong correlations were found between ICI and numerous morphological parameters.

Previous research has focused on single or multiple risk factors associated with the rupture of IAs, primarily concentrating on the patients' overall clinical attributes, the aneurysms' morphological and hemodynamic traits, or the correlations therein. It is widely recognized that, in contrast to unruptured aneurysms, ruptured aneurysms are more irregular in shape and subject to an unfavorable hemodynamic environment. These rupture-influencing factors are relevant to aneurysms found in diverse positions[8, 14–16]. Nevertheless, earlier studies also have suggested that the location of the aneurysms exerts certain impacts on their rupture[17, 18]. Consequently, it becomes imperative to recalibrate the rupture risk threshold for each parameter and take into account the location of the aneurysm when factors related to aneurysm rupture are examined.

The classification of aneurysms based on their location as sidewall or bifurcation is well-established. Doddasomayajula *et al* have reported that bifurcation aneurysms in the anterior and posterior circulations exhibit distinct rupture risks and hemodynamic characteristics[19]. However, studies have demonstrated that approximately 90% of IAs are situated in the anterior circulation, which is supplied by the ICA, while only 10% are found in the posterior circulation, supplied by the vertebrobasilar artery[20]. Consequently, this study focused exclusively on unruptured aneurysms located in the anterior circulation.

In this research, bifurcation aneurysms were predominantly distributed in the MCA (45.5%) and ACOM (45.5%). However, no significant differences were observed in the morphological or hemodynamic parameters between bifurcation aneurysms at these two sites. This finding suggests that the location does not influence the growth or rupture of bifurcation aneur-ysms in the anterior circulation, which aligns with previous research conclusions. For instance, Feng *et al* identified the bifurcation location as a crucial independent factor for the rupture risk of small unruptured IAs (<5 mm) by analyzing 618 cases of small IAs[21]. Similarly, Jing *et al* found that the location of intracranial aneurysms (sidewall/bifurcation) showed statistically significant difference in the study of multiple IA rupture risks[22]. Furthermore, Liu *et al* proposed that bifurcation was an independent risk factor for aneurysm rupture, irrespective of its location[23].

In this study, we compared the morphological parameters of sidewall and bifurcation IAs, revealing that the parent D_{vessel} of sidewall aneurysms was significantly larger than that of bifurcation aneurysms. Conversely, the θ_F and SR of sidewall aneurysms were significantly smaller than those of bifurcation aneurysms. No significant differences were observed in other morphological parameters.

Historically, aneurysm size has been considered a predictor of rupture risk[24]. However, recent studies have shown that small aneurysms still pose a certain risk of rupture, and size alone is not sufficient to accurately predict the risk of aneurysm rupture. Qiu *et al* previously suggested that the standard for aneurysm rupture is not solely based on the absolute size; rather, the size of the aneurysm relative to the parent artery is a more critical factor[25]. The SR provides a relatively straightforward method for measuring this, accounting for the maximum height of the aneurysm relative to the parent artery. SR represents the ratio of the aneurysm sac height to the average diameter of the parent artery and intuitively reflects the degree of blood vessel degradation caused by the aneurysm. Many current studies propose that SR is an independent risk factor for aneurysm rupture, with a larger SR correlating to a higher risk of rupture[15]. As SR increases, the flow pattern within the aneurysm becomes more complex, and the risk of rupture escalates[26]. The ICA, a primary branch of the anterior circulation, predominantly supplies the brain's anterior circulation. Due to its naturally larger D_{vessel} than other branches, bifurcation aneurysms exhibit a significantly larger SR than sidewall aneurysms.

The θ_F is used to represent the morphological relationship between the aneurysm and the parent artery and is considered an independent and potent discriminator for the ruptured state of sidewall aneurysms. Lv *et al* analyzed 108 aneurysms, comparing the morphological features of 68 ruptured and 40 unruptured aneurysms, and inferred that the θ_F is an independent risk factor for aneurysm rupture[27]. Tykocki *et al* also posited that the θ_F is a predictive factor for aneurysm rupture, with a high-risk threshold for rupture at 113.1°[28]. In our study, the average θ_F of bifurcation aneurysms exceeded 130°, significantly surpassing this threshold.

We performed a comprehensive statistical analysis on 4 hemodynamic parameters that are closely related to the growth and rupture of aneurysms. Our findings suggest that only bifurcation aneurysms had a significantly greater ICI than sidewall aneurysms. The other 3 parameters did not exhibit any significant differences. A study conducted by Evju *et al* in 2017 on 38 MCA bifurcation aneurysms discovered that only the ICI, among other hemodynamic indicators, showed substantial differences between ruptured and unruptured aneurysms[29]. Although the remaining hemodynamic parameters were associated with aneurysm rupture, there was no significant difference between bifurcation and sidewall aneurysms. Hence, bifurcation aneurysms with a larger ICI are at a higher risk of rupture.

Despite the significant difference in the ICI between bifurcation and sidewall aneurysms, there was a consistent correlation between morphological features and the ICI. H_{max}, H, D_{neck}, and SR of both aneurysm types significantly correlated with the ICI, indicating the intricate relationship between aneurysm morphology and hemodynamics, with several morphological parameters exerting mutual influence on the ICI. The force of blood flow impacting the vessel wall fosters aneurysm growth until rupture, with ruptured aneurysms consistently presenting a larger H_{max} than their unruptured counterparts. D_{neck} and

SR indicate the degree of aneurysm shunting on the feeding artery. As D_{neck} and SR increase, the blood flow concentration increases, thereby enhancing the impact. The θ_F, which influences the angle of blood flow entry, exhibited a weak correlation with the ICI in this study.

We identified significant associations between the SR and various hemodynamic parameters (P<0.001) in both sidewall and bifurcation aneurysms, each displaying considerable morphological disparities relative to the other. Meng *et al* proposed that a low WSS coupled with a high OSI could instigate inflammation-mediated destructive-remodeling processes, potentially linked to aneurysm rupture[5]. In addition, Qiu *et al* have documented a negative correlation between WSS and SR[25]. Similarly, Tremmel *et al* discovered that when SR surpasses 2, the proportion of the IA area subjected to a low WSS significantly escalates[26]. To enable comparison across different patients, the WSS distribution was normalized by the mean parent vessel WSS of the same patient[12]. Consequently, the negative correlation between SR and NWSS carries more weight in the study of aneurysm rupture. Consistent with our observations, we further identified significant positive correlations between the SR and the OSI as well as the ICI in both sidewall and bifurcation aneurysms. We also detected significant associations between the AR, SR, and RRT in sidewall aneurysms. RRT, initially introduced by Himburg *et al*, signifies the duration of particle proximity to the vessel wall in the bloodstream[30]. A prolonged RRT indicates an elevated duration of atherosclerotic particle exchange and monocyte recruitment in the blood, fostering atherosclerosis development and heightening aneurysm rupture risk[31]. However, the RRT in bifurcation aneurysms exhibited no correlation with any of the morphological parameters, which we hypothesize could be attributed to morphological differences in these aneurysm types. This hypothesis necessitates further validation in future studies. The correlations between the SR and these hemodynamic parameters imply their intimate connection with aneurysm rupture. Although Lauric *et al* have suggested assessing the SR based on the definition of sidewall or bifurcation aneurysms, our study affirmed that these findings apply to both bifurcation and sidewall aneurysms[32]. Moreover, the SR is an easily quantifiable parameter and therefore an important tool to quickly differentiate between sidewall and bifurcation aneurysms with different rupture risks.

There are some limitations to our study that should be addressed. Primarily, our data collection was conducted at a single center with a relatively small sample size of only 180 cases. Therefore, additional data are required to confirm our findings. Secondly, we deliberately omitted posterior circulation aneurysms to emphasize the pattern, and, concurrently, we excluded ruptured aneurysms during patient selection, a factor that hindered us from performing a comparative analysis of our findings. Additionally, our study was confined to saccular aneurysms. Future research should incorporate other types such as traumatic, infectious, dissecting, and fusiform aneurysms for further validation. Fourthly, our CFD simulations did not employ patient-specific inflow boundary conditions. Instead, we utilized rigid walls, laminar flow, and Newtonian blood flow in the CFD analysis. Moreover, we presumed a uniform wall thickness in aneurysms at varying locations. These methodologies may potentially impact the precision of our results to a certain degree.

In conclusion, the findings of this investigation indicate significant differences between sidewall and bifurcation aneurysms in anterior circulation arteries concerning morphological parameters, including D_{vessel}, θ_F, and SR, as well as the hemodynamic parameter ICI. These distinctions may explain the historically higher rupture propensity of bifurcation aneurysms and propose that these parameters warrant consideration when determining threshold differences between bifurcation and sidewall aneurysms in the context of anterior circulation aneurysm rupture risk assessment. Notably, the morphological parameter SR, which exhibits a significant correlation with various hemodynamic parameters, may serve as a valuable indicator for rapidly distinguishing the differential rupture risks associated with sidewall and bifurcation aneurysms.

Conflict of Interest Statement

The authors declare that they have no conflicts of interest.

REFERENCES

1 van Gijn J, Kerr RS, Rinkel GJE. Subarachnoid haemorrhage. The Lancet, 2007,369(9558):306-318

2 Xiang J, Yu J, Choi H, *et al*. Rupture Resemblance Score (RRS): toward risk stratification of unruptured intracranial aneurysms using hemodynamic–morphological discriminants. J Neurointerv Surg, 2015,7(7):490-495

3 Ku DN, Giddens DP, Zarins CK, *et al*. Pulsatile flow and atherosclerosis in the human carotid bifurcation. Positive correlation between plaque location and low oscillating shear stress. Arteriosclerosis, 1985,5(3):293-302

4 Qian Y, Takao H, Umezu M, *et al*. Risk analysis of unruptured aneurysms using computational fluid dynamics technology: preliminary results. Am J Neuroradiol, 2011,32(10):1948-1955

5 Meng H, Tutino VM, Xiang J, *et al*. High WSS or low WSS? Complex interactions of hemodynamics with intracranial aneurysm initiation, growth, and rupture: toward a unifying hypothesis. AJNR Am J Neuroradiol, 2014,35(7):1254-1262

6 Hassan T, Timofeev EV, Saito T, *et al*. A proposed parent vessel geometry—based categorization of

saccular intracranial aneurysms: computational flow dynamics analysis of the risk factors for lesion rupture. J Neurosurg, 2005,103(4):662-680
7 Detmer FJ, Chung BJ, Jimenez C, *et al*. Associations of hemodynamics, morphology, and patient characteristics with aneurysm rupture stratified by aneurysm location. Neuroradiology, 2019,61(3):275-284
8 Liu Q, Jiang P, Wu J, *et al*. The Morphological and Hemodynamic Characteristics of the Intraoperative Ruptured Aneurysm. Front Neurosci, 2019,13:233
9 Fahrig R, Nikolov H, Fox AJ, *et al*. A three-dimensional cerebrovascular flow phantom. Med Phys, 1999,26(8):1589-1599
10 Nambu I, Misaki K, Uchiyama N, *et al*. High Pressure in Virtual Postcoiling Model is a Predictor of Internal Carotid Artery Aneurysm Recurrence After Coiling. Neurosurgery, 2019,84(3):607-615
11 Cebral JR, Mut F, Weir J, *et al*. Quantitative characterization of the hemodynamic environment in ruptured and unruptured brain aneurysms. Am J Neuroradiol, 2011,32(1):145-151
12 Jou LD, Lee DH, Morsi H, *et al*. Wall shear stress on ruptured and unruptured intracranial aneurysms at the internal carotid artery. Am J Neuroradiol, 2008,29(9):1761-1767
13 He X, Ku DN. Pulsatile flow in the human left coronary artery bifurcation: average conditions. J Biomech Eng, 1996,118(1):74-82
14 Sheikh MAA, Shuib AS, Mohyi MHH. A review of hemodynamic parameters in cerebral aneurysm. Interdiscip Neurosur, 2020,22
15 Zhang J, Can A, Mukundan S, *et al*. Morphological Variables Associated With Ruptured Middle Cerebral Artery Aneurysms. Neurosurgery, 2019,85(1):75-83
16 Lv N, Karmonik C, Chen S, *et al*. Wall Enhancement, Hemodynamics, and Morphology in Unruptured Intracranial Aneurysms with High Rupture Risk. Transl Stroke Res, 2020,11(5):882-889
17 Brown RD, Broderick JP. Unruptured intracranial aneurysms: epidemiology, natural history, management options, and familial screening. Lancet Neurol, 2014,13(4):393-404
18 Gross BA, Lai PMR, Du R. Impact of aneurysm location on hemorrhage risk. Clin Neurol Neurosur, 2014,123:78-82
19 Doddasomayajula R, Chung B, Hamzei-Sichani F, *et al*. Differences in Hemodynamics and Rupture Rate of Aneurysms at the Bifurcation of the Basilar and Internal Carotid Arteries. Am J Neuroradiol, 2017,38(3):570-576
20 Wiebers DO, Whisnant JP, Huston J, 3rd, *et al*. Unruptured intracranial aneurysms: natural history, clinical outcome, and risks of surgical and endovascular treatment. Lancet, 2003,362(9378):103-110
21 Feng X, Ji W, Qian Z, *et al*. Bifurcation Location Is Significantly Associated with Rupture of Small Intracranial Aneurysms (<5 mm). World Neurosurg, 2017,98:538-545
22 Jing L, Fan J, Wang Y, *et al*. Morphologic and Hemodynamic Analysis in the Patients with Multiple Intracranial Aneurysms: Ruptured versus Unruptured. PLoS One, 2015,10(7):e0132494
23 Liu Q, Jiang P, Jiang Y, *et al*. Bifurcation Configuration Is an Independent Risk Factor for Aneurysm Rupture Irrespective of Location. Front Neurol, 2019,10:844
24 Forget Jr TR, Benitez R, Veznedaroglu E, *et al*. A review of size and location of ruptured intracranial aneurysms. Neurosurgery, 2001,49(6):1322-1326
25 Qiu T, Xing H. Morphological Distinguish of Rupture Status between Sidewall and Bifurcation Cerebral Aneurysms. Int J Morphol, 2014,32(3):1111-1119
26 Tremmel M, Dhar S, Levy EI, *et al*. Influence of intracranial aneurysm-to-parent vessel size ratio on hemodynamics and implication for rupture: results from a virtual experimental study. Neurosurgery, 2009,64(4):622-630
27 Lv N, Feng Z, Wang C, *et al*. Morphological Risk Factors for Rupture of Small (<7 mm) Posterior Communicating Artery Aneurysms. World Neurosurg, 2016,87:311-315
28 Tykocki T, Nauman P, Dow Enko A. Morphometric predictors of posterior circulation aneurysms risk rupture. Neurol Res, 2014,36(8):733-738
29 Evju O, Pozo JM, Frangi AF, *et al*. Robustness of common hemodynamic indicators with respect to numerical resolution in 38 middle cerebral artery aneurysms. PLoS One, 2017,12(6):e0177566
30 Himburg HA, Grzybowski DM, Hazel AL, *et al*. Spatial comparison between wall shear stress measures and porcine arterial endothelial permeability. Am J Physiol-Heart C, 2004,286(5):H1916-H1922
31 Sugiyama S, Niizuma K, Nakayama T, *et al*. Relative residence time prolongation in intracranial aneurysms: a possible association with atherosclerosis. Neurosurgery, 2013,73(5):767-776
32 Lauric A, Baharoglu MI, Malek AM. Size ratio performance in detecting cerebral aneurysm rupture status is insensitive to small vessel removal. Neurosurgery, 2013,72(4):547-554

(Received Dec. 13, 2023; accepted Jan. 16, 2024)